RSC Advances

PAPER

View Article Online
View Journal | View Issue

Cite this: *RSC Adv.*, 2017, **7**, 18189

Effects of the acceptor pattern and substitution position on the properties of *N*-phenyl-carbazolyl based donor–acceptor–donor molecules†

Xuejing Song,[a] Min Wang,[b] Lingqian Kong[c] and Jinsheng Zhao *[d]

Four optoelectronic compounds based on the same donor (*N*-phenylcarbazole) and different acceptors of benzothiadiazole or benzoselenadiazole were designed and synthesized to investigate the effects of the substitution position and effects of the acceptor heteroatom on the properties of *N*-phenyl-carbazolyl based organic optoelectronic compounds. The results demonstrated that these four compounds have band gaps (2.25 to 2.59 eV) that are lower than that of carbazole (3.20 eV). For the acceptor moiety, the replacement of benzothiadiazole with benzoselenadiazole was beneficial for the polarization of the D–A compound. Different acceptors substituted at the 3-position of *N*-phenylcarbazole led to molecules with a higher degree of planar conjugation than molecules derived from acceptors substituted at the 2-position. The increase in polarity and conjugation degree of the D–A compounds gave rise to lower band gaps and redshifts in the UV-vis absorption spectra and fluorescence emission spectra compared to the corresponding compounds. Solvatochromism effects were observed for these four compounds in different polar solvents, accompanied by redshifts in the fluorescence emission spectra, which ranged from 509 nm to 596 nm. Using thermogravimetric analysis, the decomposition temperatures of all four materials were found to be above 400 °C.

Received 4th February 2017
Accepted 18th March 2017

DOI: 10.1039/c7ra01449j

rsc.li/rsc-advances

Introduction

Carbazole is an industrial raw material that is inexpensive and available in large quantities. Carbazole and its derivatives can be fused with many aromatic units to generate novel compounds,[1] which have applications in a variety of fields, such as in photoelectric materials,[2,3] dyes,[4,5] medicines[6] and biosensors.[7] For carbazole, facile substituted modification on the 9′-nitrogen atom and optional link of the 2′- or 3′-sites enable the precise regulation of the band gaps of the resultant molecule.[4] The important merits of carbazole derivatives include their high hole mobilities, perfect luminous performance, high molar extinction coefficients and capacity to undergo polymerization.[8]

Donor (D)–acceptor (A)-type compounds usually have low band gaps due to the push–pull effect along the molecular skeleton; these molecules have become an increasingly important class of conjugated materials.[9–15] Carbazole and its derivatives are frequently used as end-capping donor units due to their strong electron-donating abilities and the obtained molecules often have fluorescence properties.[16–18] Przemyslaw Ledwon *et al.* synthesized a compound with a D–π–A–π–D structure employing carbazole as the D unit, benzothiadiazole (BTD) as the A unit, and 2-vinyl-3-hexyl-thiophene as the π linker; the molecule has a unique deep red color and is infrared emitting.[8]

As a strongly electron deficient unit, BTD is frequently used for the construction of D–A type conjugated molecules. Some of the resultant molecules have light-emitting properties and can be used as active materials in many fields, including heavy metal ion assay,[14,15] biosensors and florescence imaging probes.[18–20] Pei jian group prepared a series of D–A–D type oligomers taking BTD as the acceptor and oligo(thienylene vinylene)s with distinct lengths as the donor unit, which showed the broad absorption bands between 300–800 nm, and their emission bands were centered at approximately 650 nm.[21] Sanjio S. Zade *et al.* reported three BTD derivatives with the D–A–D configuration and phenyl, thiophene and selenophene as the donor units. Respectively, the emissive colours of the three molecules were green (phenyl), orange (thiophene) and red (selenophene).[22] In brief, the properties of D–A type materials depend on the proper combination of the A unit and D unit, as well as the substitution sites.[23]

Benzoselenadiazole (BSe) is an analogue of BTD, that is obtained by replacing an S atom with an Se.[24] The selenium atom has a larger size and is less electronegative than sulphur.[25] Therefore, BSe-containing compounds usually have red shifts in both absorption spectra and fluorescence-emitting spectra

[a]*Dongguan University of Technology, Dongguan, 523808, P. R. China*
[b]*Liaocheng Pepole's Hospital, Liaocheng, 252000, P. R. China*
[c]*Dongchang College, Liaocheng University, 252059, P. R. China*
[d]*Department of Chemistry, Liaocheng University, Liaocheng, 252059, P. R. China. E-mail: zhaojinsheng@lcu.edu.cn; Fax: +86-635-8539607; Tel: +86-635-8539607*

† Electronic supplementary information (ESI) available. See DOI: 10.1039/c7ra01449j

relative to the corresponding BTD-containing compounds.[24,25] A series of dyes were designed and synthesized using 5-thienyl-BTD or 5-thienyl-BDS as the electron-deficient cores the fluorene derivatives as the D units. The resultant compounds had valuable NIR emission properties with high quantum yields.[20] The replacement of the BTD unit with a BDS unit also shifted the absorption of the molecules toward longer wavelengths.[20]

There are no reports concerning the direct combination of *N*-phenylcarbazole with BTD for the construction of D–A–D-type materials; novel fluorescent dyes with a high performance could be anticipated for such a combination. The effects of the replacement of BTD by BSe on the fluorescence properties of the obtained D–A–D-type molecules also deserve study. Changes in the substitution positions on the carbazole derivative units would also have a direct influence on the properties of the resultant compounds and still need to be studied. Based on these considerations, we present in this study the synthesis of four D–A–D-type analogous molecules employing *N*-phenylcarbazole and benzothiadiazole (or benzoselenadiazole) as the D and A units, respectively, with the aim of exploring the effects of the substitution positions and heteroatom replacement within the acceptor units on the properties of the obtained substance.[26] Their specific properties, including optical, redox and thermal stabilities, were studied in detail. Interestingly, the fluorescent dyes obtained emitted yellow, green and red colours upon irradiation, that is, the primary colours. Any colour can be made from these primary colours, which makes them important and leads them to have wide application prospects in the organic electroluminescent field. All of the compounds showed the solvatochromism effect in different polar solvents and had simultaneous high thermal stability and redox activities. As anticipated, the replacement of BTD by BSe as the acceptor unit could also reduce the band gap of the resultant molecules.

Experimental

Materials

2-Boric acid-*N*-phenylcarbazole (98%), 3-boric acid-*N*-phenylcarbazole (98%), 4,7-bibromine-2,1,3-benzothiadiazole (98%), sodium borohydride ($NaBH_4$, 98%), sodium carbonate (Na_2CO_3, 98%), selenium dioxide (SeO_2, 99%), tetra (triphenylphosphine) palladium ($Pd(PPh_3)_4$), tetra-*n*-butylammonium fluoride (TBAF), ethanol (EtOH, 99.9%), methylbenzene (AR), *n*-hexane (AR), trichloromethane (AR), *N*,*N*-dimethylformamide (DMF, AR), methanol (AR), dimethyl sulfoxide (AR) and anhydrous magnesium sulphate (AR) were all purchased from the Aldrich Chemical Reagent Company and used directly without further treatment. Tetrabutylammonium hexafluorophosphate ($TBAPF_6$, 98%) was purchased from Alfa Aesar. Thin layer chromatography (TLC) silica gel (GF254) and column layer chromatography silica gel (200–300 meshes) were provided by Qingdao Marine Chemical Factory.

Characterization

^1H and ^{13}C NMR were recorded using a Varian AMX 400 nuclear magnetic resonance spectrometer ($CDCl_3$, 400 MHz), and tetramethylsilane was used as the internal standard substance. Elemental analysis was performed on a Thermo Finnigan Flash EA 1112 analyser. MALDI-TOF MS spectra were recorded using Bruker Daltonics Flexanalysis.

UV-vis absorption spectra were collected by Varian Cary 5000 spectrometer. A serials of solvents including *n*-hexane, dichloromethane, trichloromethane, methylbenzene, tetrahydrofuran, acetonitrile, DMF, methanol and dimethyl sulfoxide were used as the solvent to prepare solutions. The D–A–D compounds, including 4,7-bis(9-phenyl-9*H*-carbazole-2-yl) benzo[*c*][1,2,5] thiadiazole (BPC-2BTD), 4,7-bis(9-phenyl-9*H*-carbazole-2-yl)benzo[*c*][1,2,5]selenadiazole (BPC-2BSe), 4,7-bis(9-phenyl-9*H*-carbazole-3-yl)thiadiazole (BPC-3BTD) and 4,7-bis (9-phenyl-9*H*-carbazole-3-yl)selenadiazole (BPC-3BSe), were dissolved in the above solvents to a respectively, with the determined concentration of 1×10^{-5} mol L^{-1}. The prepared solutions were undertaken for UV-vis measurement with a scan range of 200–800 nm.

Fluorescence spectra were measured on a LS55 fluorescence photometer (Perkin Elmer). The fluorescence emission spectra of the compounds were measured using a 1 cm standard quartz cuvette with a slit width of 6.0 nm, appropriate excitation wavelength, a voltage of 700 V and a scanning speed of 300 nm min^{-1}. The redox property of the compounds was studied using cyclic voltammetry method in a dry DCM solution containing 0.2 M $TBAPF_6$. A three-electrode system was employed with a Pt wire (Φ 0.5 mm) as the working electrode, a Pt ring (Φ 0.5 mm) as the counter electrode, and a Ag/AgCl electrode as the reference electrode. The thermal stabilities of compounds were tested using a NETZSCH STA 499C TG-DSC tester under an N_2 atmosphere, temperature range of 40–800 °C, and heating rate of 10 °C min^{-1}. A Canon Power Shot A3000 IS was used to take pictures of the four compounds and its solutions and their solutions.

Synthesis of acceptor unit

The acceptor unit 4,7-dibromo-2,1,3-benzoselenadiazole was synthesized using the methods reported previously in the literature[24–28] (Scheme 1(a)): 5.75 g (19.56 mM) of 4,7-dibromo-2,1,3-benzothiadiazole and 300 mL of ethanol were added into a 500 mL three-necked flask in a thermostat water bath. Under electromagnetic stirring at 30 °C, an excessive of 16 g (422 mM) $NaBH_4$ was added to the above suspension in three portions over an interval of 8 h. Forty-eight hours later, the reaction was terminated by pouring the mixture directly into 500 mL of distilled water; abundant white floccules precipitated. The mixture was stirred mechanically for 5 min and filtered by decompression suction to afford white solid 3,6-dibromo-1,2-phenylenediamine. The solid was dried in a vacuum oven for 20 hours and reserved for further application. ^1H NMR ($CDCl_3$, 400 MHz, ppm): $\delta = 6.84$ (s, 2H, Ar H), 3.89 (s, 4H). ^{13}C NMR ($CDCl_3$, δ, ppm): $\delta = 133.70$, 123.24, 109.68.

To prepare 4,7-dibromo-2,1,3-benzoselenadiazole, 9.47 g (36.91 mM) 3,6-dibromo-1,2-phenylenediamine was dissolved in 200 mL ethyl alcohol in a flask, and the solution was heated to 90 °C in a water bath. At the same time, 4.2 g of SeO_2 (37.85

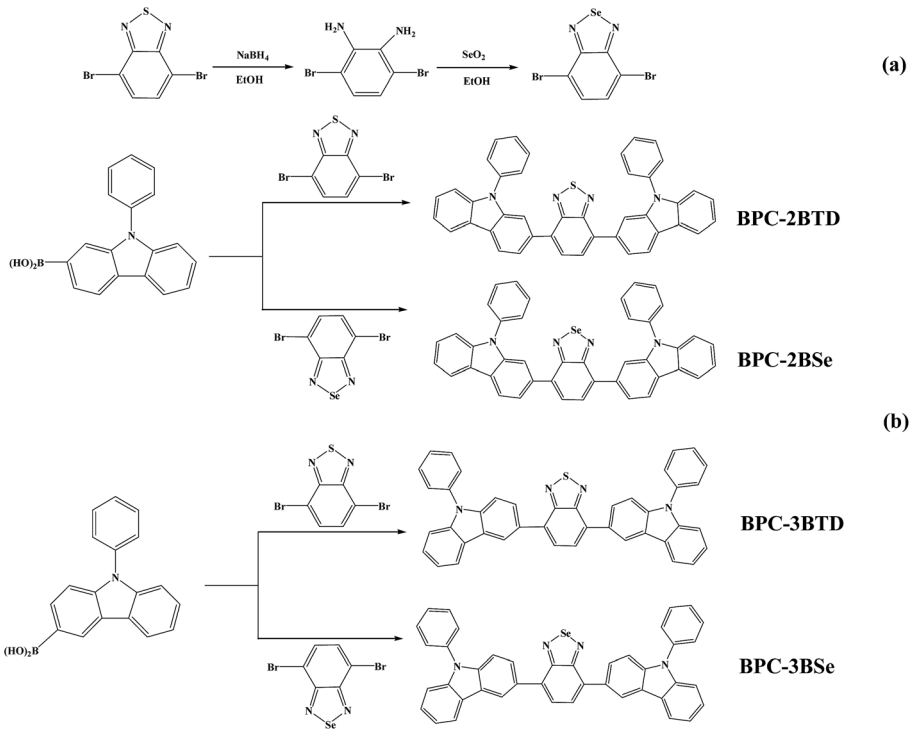

Scheme 1 Synthetic routes of acceptor and four D–A–D compounds.

mM) was dissolved into 50 mL hot water, and the solution was added to the reaction flask slowly. Yellow insoluble substances were produced. The mixture was refluxed for 2 h, and 4,7-dibromo-2,1,3-benzoselenadiazole was afforded from vacuum filtration.[28] The yellow solid was then washed with ethanol three times, with water three times and dried under vacuum at 50 °C. ^{1}H NMR ($CDCl_3$, 400 M Hz, ppm): δ = 7.64 (s, 2H, Ar H). ^{13}C NMR ($CDCl_3$, δ, ppm): δ = 158.16, 144.00, 139.30.

Synthesis of D–A–D compounds

The synthetic routes are outlined in Scheme 1(b). Four molecules including BPC-2BTD, BPC-2BSe, BPC-3BTD and BPC-3BSe were synthesized using Suzuki coupling reactions.[29] The specific synthetic process for BPC-2BTD was as follows: 3 g of (10.45 mM) 2-boric acid-*N*-phenylcarbazole, 1.53 g of (5.22 mM) 4,7-dibromo-2,1,3-benzoselenadiazole, 40 mL of (2 mol L^{-1}) $NaCO_3$ solution and 60 mL of methylbenzene (volume ratio of methylbenzene and $NaCO_3$ was 3 : 2) were added into a round-bottom flask. Then, 0.6 g of $Pd(PPh_3)_4$ (molar mass of reactant was 5%) and 0.1 g of phase transfer agent TBAF were added to the flask. The flask was subjected to gas displacement until the atmosphere in the flask was replaced by argon gas. The flask was stirred magnetically under argon, heated to 120 °C and maintained for 48 h. After the reaction was completed, the solvent was removed under vacuum. The residue was dissolved in DCM, washed three times with water and dried over magnesium sulphate. The resulting crude product was obtained by distillation of the solvent, and purified using column chromatography (3 : 1, *n*-hexane, dichloromethane). Finally, 2.2 g of yellow powder was collected (yield of 68%), and termed BPC-2BTD. ^{1}H NMR ($CDCl_3$, 400 MHz, ppm): δ = 8.27 (d, 2H, ArH), 8.19 (d, 2H), 7.97 (d, 2H), 7.88 (d, 2H), 7.78 (s, 2H), 7.60 (m, 8H), 7.44 (m, 6H), 7.31 (m, 2H) (see Fig. S1a in ESI†). ^{13}C NMR ($CDCl_3$, δ, ppm): δ = 158.90, 146.13, 145.69, 142.16, 139.97, 138.42, 134.54, 132.96, 132.12, 131.77, 130.84, 128.00, 127.74, 126.07, 125.15, 124.96, 124.75, 115.27, 114.48 (see Fig. S1b in ESI†). MS (MALDI-TOF): *m*/*z*: calcd for 618.19; found 618.75. Elemental analysis calcd (%): C 81.53, H 4.24, N 9.05, S 5.18; found: C 81.35, H 4.27, N 9.13, S 5.25.

The synthesis of BPC-2BSe was the same as for BPC-2BTD, which was obtained as a fluffy yellow solid with a yield of 71%. ^{1}H NMR ($CDCl_3$, 400 MHz, ppm): δ = 8.26 (d, 2H, ArH), 8.18 (d, 2H), 7.86 (d, 2H), 7.80 (d, 2H), 7.62 (s, 2H), 7.58 (m, 8H), 7.43 (m, 6H), 7.30 (m, 2H) (see Fig. S2a in ESI†). ^{13}C NMR ($CDCl_3$, δ, ppm): δ = 159.88, 141.43, 140.96, 137.53, 135.95, 135.60, 129.86, 128.68, 127.43, 127.12, 126.11, 123.26, 123.12, 121.73, 120.47, 120.12, 120.06, 110.76, 109.80 (see Fig. S2b in ESI†). MS (MALDI-TOF): *m*/*z*: calcd for 666.13; found 666.17. Elemental analysis calcd (%): C 75.78, H 3.94, N 8.42, Se 11.86; found: C 75.56, H 4.00, N 8.48, Se 11.96.

BPC-3BTD was obtained as a the yellow solid with a yield of 72%, and the procedure used was the same as the above two compounds. ^{1}H NMR ($CDCl_3$, 400 MHz, ppm): δ = 8.75 (d, 2H, ArH), 8.25 (d, 2H), 8.04 (d, 2H), 7.85 (s, 2H), 7.61 (m, 8H), 7.55 (d, 2H), 7.46 (m, 6H), 7.33 (m, 2H) (see Fig. S3a in ESI†). ^{13}C NMR ($CDCl_3$, δ, ppm): δ = 154.52, 141.31, 140.75, 137.51, 133.21, 129.91, 129.58, 127.96, 127.55, 127.43, 127.06, 126.17, 123.70, 123.53, 121.20, 120.56, 120.16, 109.94, 109.83 (see Fig. S3b in ESI†). MS (MALDI-TOF): *m*/*z*: calcd for 618.19; found 618.33. Elemental analysis calcd (%): C 81.53, H 4.24, N 9.05, S 5.18; found: C 81.41, H 4.24, N 9.15, S 5.20.

Similarly, the fourth compound BPC-3BSe was produced as a reddish-orange solid in a yield of 68.7%. ^{1}H NMR ($CDCl_3$, 400 MHz, ppm): $\delta = 8.68$ (d, 2H, ArH), 8.25 (d, 2H), 8.00 (q, 2H), 7.76 (s, 2H), 7.64 (m, 8H), 7.57 (d, 2H), 7.48 (m, 6H), 7.34 (m, 2H) (see Fig. S4a in ESI†). ^{13}C NMR ($CDCl_3$, δ, ppm): $\delta = 160.26$, 141.30, 140.71, 137.53, 135.14, 130.19, 129.90, 128.40, 127.71, 127.55, 127.09, 126.11, 123.58, 123.50, 121.38, 120.53, 120.09, 109.90, 109.67 (see Fig. S4b in ESI†). MS (MALDI-TOF): *m*/*z*: calcd for 666.13; found 666.25. Elemental analysis calcd (%): C 75.78, H 3.94, N 8.42, Se 11.86; found: C 75.59, H 3.98, N 8.53, Se 11.90.

Results and discussion

Synthesis and characterization

The general synthetic method of acceptor unit 4,7-dibromo-2,1,3-benzoselenadiazole and four D–A–D compounds is shown in Scheme 1. In the ethanolic solution, 4,7-dibromo-2,1,3-benzothiadiazole reacted with $NaBH_4$ to produce 3,6-dibromo-1,2-phenylenediamine at a yield of 75%. SeO_2 was dissolved in hot water and added to an ethanol solution of 3,6-dibromo-1,2-phenylenediamine to produce the acceptor unit 4,7-dibromo-2,1,3-benzoselenadiazole (yield of 62%). Four analogous D–A–D compounds (BPC-2BTD, BPC-2BSe, BPC-3BTD and BPC-3BSe) were synthesized using Suzuki coupling reactions between 2-boric acid-*N*-phenylcarbazole (as electron donor) and 4,7-bibromine-2,1,3-benzothiadiazole or 4,7-dibromo-2,1,3-benzoselenadiazole (as electron acceptor) at a high yield. The four compounds exhibited high solubility in common solvents, including hexane, dichloromethane, chloroform, toluene and tetrahydrofuran, *etc.* The obtained compounds were confirmed by ^{1}H NMR, ^{13}C NMR spectroscopy, mass spectroscopy and elemental analysis.

UV-vis absorption spectra

The UV-vis absorption spectra of four compounds in various solvents were analyzed; the results are shown in Fig. 1.

In Fig. 1, all of the compounds showed two characteristic absorption bands in all of the solvents. There was one intense absorption at short wavelength and a second weak absorption at long wavelengths. The short wavelength absorption bands were attributed to π–π^* transitions in the *N*-phenylcarbazole moieties, and the long wavelength absorption bands were assigned to the intramolecular charge-transfer (ICT) from the electron-donating *N*-phenylcarbazole moiety to the central electron-withdrawing group, that is BTD or BSe.[24,25] The UV-vis absorption spectra of each compound in different solutions are similar, but slightly solvent-dependent. With increased solvent polarity, the absorption bands of four compounds showed slight redshifting (less than 10 nm), indicating a slight solvatochromic effect in the ground state of four compounds. The positions of the characteristic absorption peaks in Fig. 1 are given in Table 1.

The UV-vis absorption spectra of four compounds in dichloromethane are discussed as an example. The absorption maxima of BPC-2BTD were located at 318 nm and 414 nm, while those of BPC-2BSe were located at 327 nm and 438 nm. The two characteristic absorption bands of BPC-2BSe were redshifted by 9 nm and 24 nm compared with those of BPC-2BTD, respectively. The same phenomenon was observed between BPC-3BTD and BPC-3BSe. The Se atom is larger in size than the S atom and less electronegative than the S atom. Thus, the Se atom exerts a weaker binding force on external electrons.[24–26] Therefore, the molecular polarization was intensified when the heteroatom S in the acceptor unit was replaced by Se. The excited state energies of BPC-2BSe and BPC-3BSe in a polar solvent were lower than those of BPC-2BTD and BPC-3BTD, respectively, leading to a redshift in the both high and low energy absorption bands.

The changes of the substitution positions may also have an effect on the absorption properties of the compounds. It was observed that the short wavelength absorption maximum of BPC-3BTD was blueshifted (20 nm) compared to that of BPC-2BTD, while the long wavelength absorption maximum was simultaneously redshifted (19 nm). The same phenomenon was observed between BPC-2BSe and BPC-3BSe. Two characteristic absorption bands moved in different directions, caused by their different transition mechanisms. The short wavelength absorption bands were mainly attributed to the π–π^* transition of the *N*-phenylcarbazole unit in the D–A–D type molecule, whereas the low energy absorption bands were caused by the ICT between the donor and acceptor units.[26]

The 3-position substitution molecules including BPC-3BTD and BPC-3BSe, appear to have better coplanarity than their corresponding analogues BPC-2BTD and BPC-2BSe, as further confirmed by the quantum chemistry calculation method in the following section. The less twisted conjugationed structure of BPC-3BTD or BPC-3BSe as compared to their respective isomers BPC-2BTD or BPC-2BSe, resulted in more effective conjugation and stronger ICT interactions. Consequently, the electron cloud densities of the *N*-phenylcarbazole units substituted at the 3-position were reduced moderately more than the *N*-phenylcarbazole unit substituted at the 2-position. This led to a blue shift of the high energy absorption bands of BPC-3BTD or BPC-3BSe compared with their respective analogues. As mentioned above, the low-energy absorption bands were caused by ICT, and the stronger ICT within the 3-position-substituted molecules than their respective analogues (2-position) caused a redshift of low-energy absorption bands. Based on the low energy absorption edges (λ_{onset}) in the UV-vis absorption spectra, the optical band gaps (E_g, $E_g = 1241/\lambda_{onset}$) of BPC-2BTD, BPC-2BSe, BPC-3BTD and BPC-3BSe were calculated to be 2.59 eV, 2.45 eV, 2.48 eV and 2.33 eV, respectively. Furthermore, it was observed that the band gaps of the 3-position substitution products were slightly lower than those of the 2-position substitution products. According to the literature, the band gap of carbazole is 3.20 eV,[30] and the D–A–D compounds reported in the present study achieved far lower band gaps than this value. This proves that building a D–A–D conjugation system by introducing acceptor units between Bi–*N*-phenylcarbazole is beneficial for reducing the band gap of carbazole derivatives.

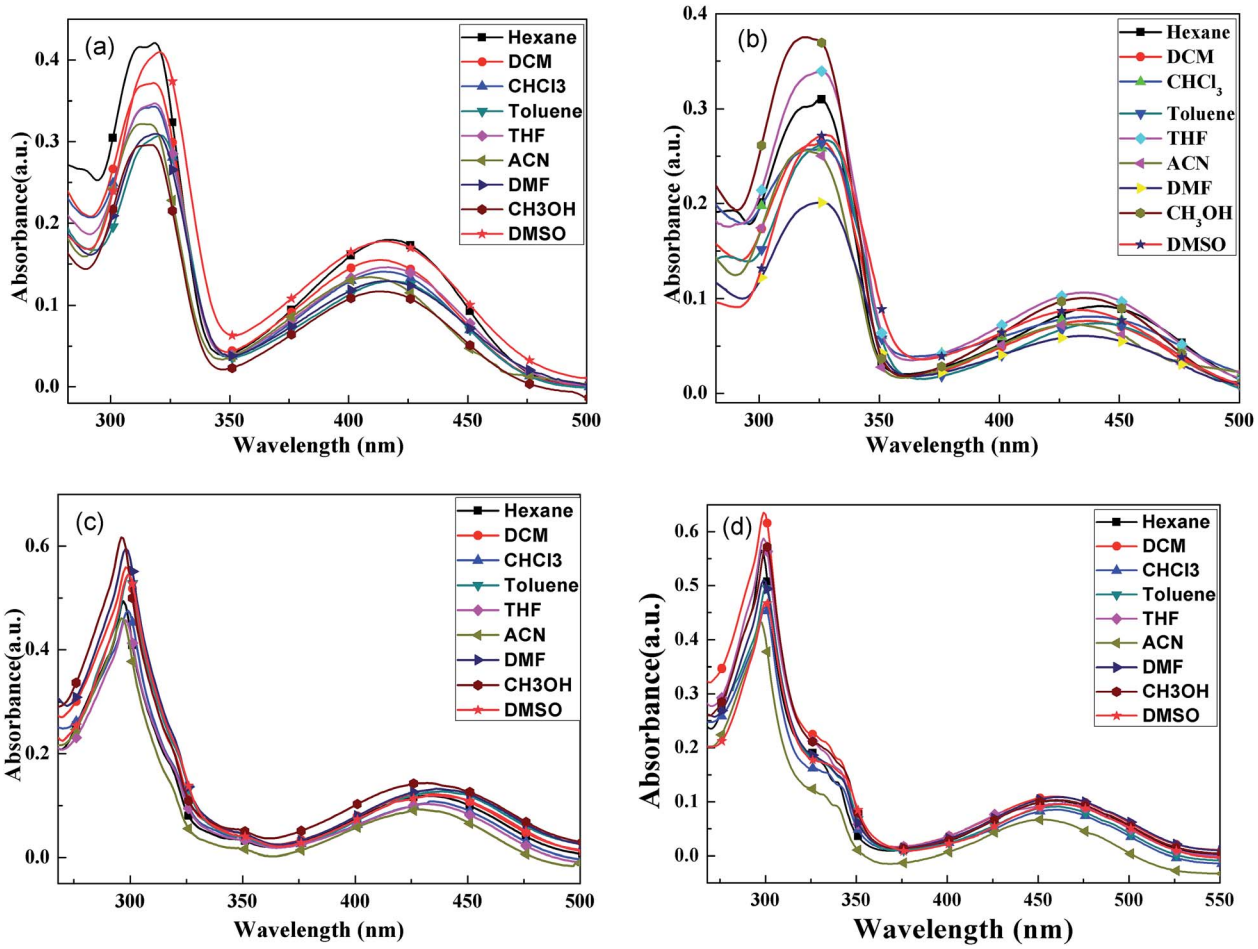

Fig. 1 UV-vis absorption spectra of BPC-2BTD (a), BPC-2BSe (b), BPC-3BTD (c) and BPC-3BSe (d) in different solvents.

Table 1 The max absorption wavelengths of BPC-2BTD, BPC-2BSe, BPC-3BTD and BPC-3BSe in different solvents

Solvent λ_{max}/nm	BPC-2BTD	BPC-2BSe	BPC-3BTD	BPC-3BSe
Hexane	317, 414	326, 438	297, 432	298, 459
Dichloromethane	318, 414	327, 438	298, 433	299, 460
Chloroform	318, 415	327, 437	299, 434	300, 461
Toluene	321, 417	329, 442	299, 439	300, 462
Tetrahydrofuran	318, 416	326, 436	298, 431	299, 460
Acetonitrile	317, 409	319, 432	296, 429	297, 453
Dimethyl formamide	319, 416	325, 436	298, 436	299, 462
Methanol	317, 413	319, 435	297, 432	300, 460
Dimethyl sulfoxide	321, 416	328, 441	300, 436	300, 463

Fluorescence emission spectra

The fluorescence emission spectra of BPC-2BTD, the fluorescence emission spectra of BPC-2BTD, BPC-2BSe, BPC-3BTD and BPC-3BSe in different solvents are shown in Fig. 2.

The fluorescence emission spectra of four compounds are similar with each other in different solvents. Unlike the UV-vis absorption spectra, all of the fluorescence emission curves of the D–A–D compounds demonstrate only one resolved ICT emission and showed a strong solvent dependence. With the increase in solvent polarity, the emission peaks exhibited large redshifts (ranging from 31 to 58 nm), displaying a significant solvatochromic effect.[31–34] This phenomenon might be related to the inherent ICT in the D–A molecules. Many studies have shown that ICT was strengthened upon excitation, which increases the molecular dipole moment.[30,31] The dipole moment in the excited state is greater than that of the molecule in the ground state. The increase in solvent polarity is beneficial for electron delocalization and the stabilization of the molecule in the excited state. The stability of the molecule in the excited state is enhanced by the increase in solvent polarity, thereby reducing the energy level of the excited state and making the energy gap between the excited state and ground state smaller. Thus, the fluorescence emission wavelength has a large redshift.[35]

Additionally, the fluorescence emission spectra of four compounds in methanol solvent were approximately straight lines without distinct emission peaks. This is because the hydrogen-bond interaction between the solvent and molecules quenched the fluorescence completely.[36] The maxima emission wavelength data of the fluorescence emission spectra are listed in Table 2.

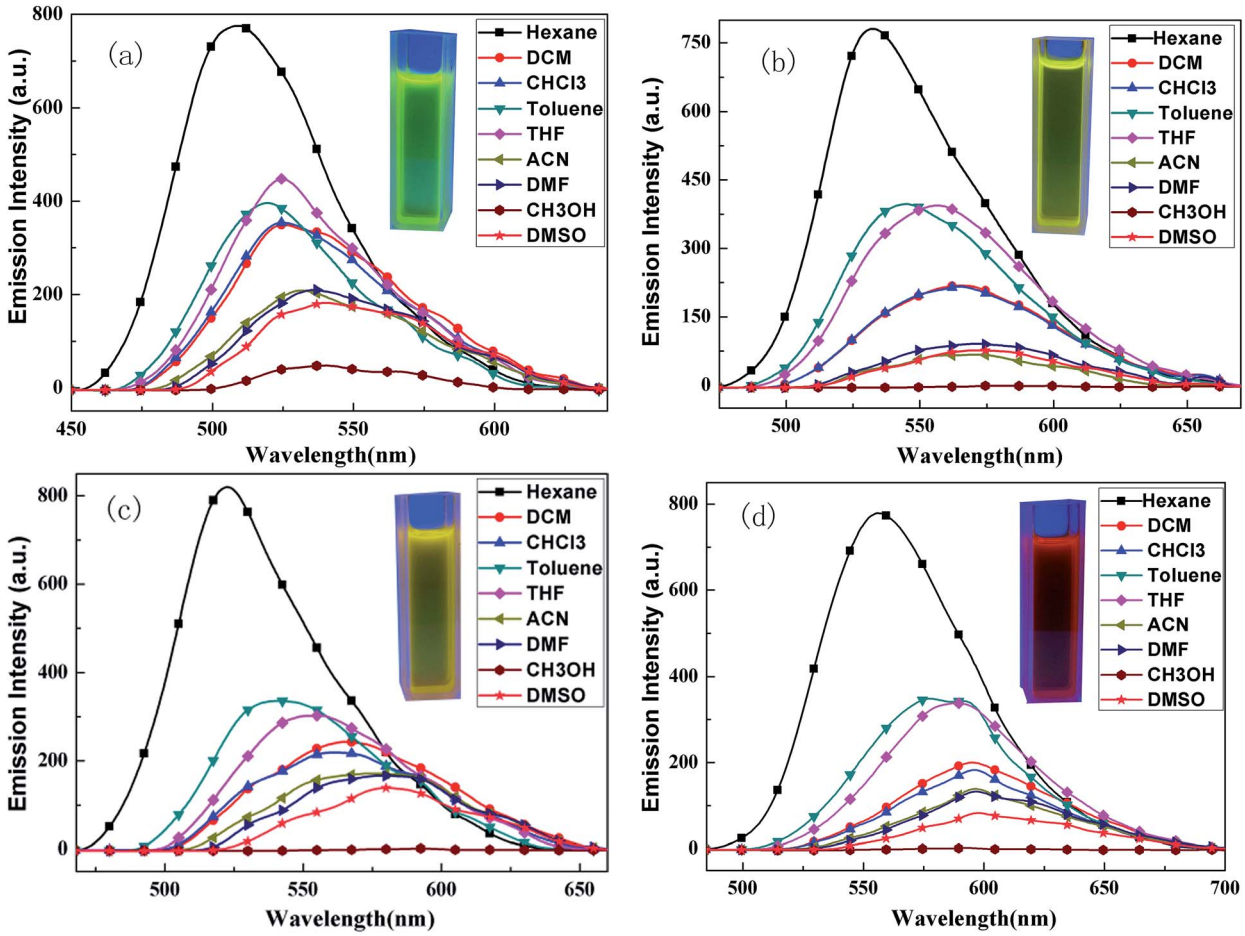

Fig. 2 Fluorescence spectra of BPC-2BTD (a), BPC-2BSe (b), BPC-3BTD (c) and BPC-3BSe (d) in different solvents. Photos show DCM solutions of four D–A–D compounds illuminated by ultraviolet light at 360 nm.

Table 2 The max fluorescence emission wavelengths of BPC-2BTD, BPC-2BSe, BPC-3BTD and BPC-3BSe in different solvents

Solvent λ_{max}/nm	BPC-2BTD	BPC-2BSe	BPC-3BTD	BPC-3BSe
Hexane	509	532	522	556
Dichloromethane	525	565	565	595
Chloroform	525	565	562	596
Toluene	520	545	540	577
Tetrahydrofuran	524	556	555	588
Acetonitrile	532	572	575	597
Dimethyl formamide	536	571	578	597
Methanol	—	—	—	—
Dimethyl sulfoxide	540	570	580	598

The fluorescence emission spectra of four compounds in dichloromethane are discussed in detail for the sake of contrast. The emission maxima of BPC-2BTD and BPC-2BSe were located at 525 nm and 565 nm, respectively. An apparent redshift of 40 nm was observed for BPC-2BSe relative to that of BPC-2BTD. Similarly, the emission band of BPC-3BSe had a redshift of 30 nm compared to that of BPC-3BTD. The cause of this phenomenon was similar to the redshift of the UV-vis absorption spectra. Replacing the heteroatom S with Se was beneficial for molecular polarization and resulted in a lower excited state energy in the polar solvent, leading to a lower band gap and a redshift of the emission wavelength. With the same acceptor unit but a different position of the substituent, the emission peak of BPC-3BTD was 565 nm, which had a redshift by 40 nm compared to BPC-2BTD. The same tendency was observed between BPC-3BSe and BPC-2BSe. This is consistent with the trend in their absorption spectra and originates from the much stronger ICT interactions in compounds BPC-3BTD and BPC-3BSe compared to their isomers, BPC-2BTD and BPC-2BSe.

Fluorescence yield

The compound 4-methylamino-7-nitro-2,1,3-benzodioxazole (NBD) was used as a reference and has fluorescence quantum yield (FQE) of 0.38 in acetonitrile.[37,38] Based on this criterion, the FQE values of the four molecules were measured in dichloromethane. Under the same conditions (fluorescence scanning range: 300–700 nm; slit width: 6.0 nm; voltage: 700 V; scanning speed: 300 nm min^{-1}), the fluorescence emission spectra of the test compounds and the reference were scanned

and their integral fluorescence intensities were calculated. Then, the FQE values of different compounds were calculated from eqn (1). The results are shown in Table 3.

$$\Phi_x = \Phi_s \left(\frac{F_x}{F_s}\right)\left(\frac{A_s}{A_x}\right)\left(\frac{n_x}{n_s}\right)^2 \quad (1)$$

where Φ_x and Φ_s are the FQE values of the testing compounds and reference; F_x and F_s are the integral fluorescence intensities of the testing compounds and reference; A_x and A_s are absorbance of the testing compounds and reference at exciting wavelength; and n_x and n_s are refractive indexes of the solvents of the testing materials and reference, respectively.

Table 3 gives the FQE values of four compounds. BPC-2BSe had a lower fluorescence efficiency than BPC-2BTD. Similarly, the fluorescence efficiency of BPC-3BSe was lower than that of BPC-3BTD. The Se atom has a larger molecular weight than the S atom, which might exert a heavy atom effect on the energy level transitions.[24,26] For example, when the singlet state in the excited state transforms into the triplet state, it cannot expediently return to the ground state through intersystem crossing due to the presence of the large Se atom. Therefore, the fluorescence efficiencies of the compounds using BSe as the acceptor were lower than for compounds using BTD as acceptor. By comparing the same acceptor pattern (BPC-3BTD and BPC-2BTD or BPC-3Be and BPC-2Be), substitution at the 2-position of *N*-phenylcarbazole had higher fluorescence luminous efficiencies than the molecules with a 3-position substitution pattern. This was caused by the large steric hindrance of substitution at the 2-position. Higher molecular rigidity is beneficial for increasing fluorescence efficiency.[23–27]

Electrochemical properties

The electrochemical properties of the compounds were tested by Cyclic Voltammetry (CV). CV curves of four compounds are presented in Fig. 3.

For BPC-2BTD, there are two irreversible redox peaks located at 1.63 V/1.04 V and an additional weak reduction peak was observed at 0.12 V. There are no any apparent redox peaks observed in the negative scan up to −1.60 V. For BPC-2BSe, only one oxidation peak was observed at a potential of 1.62 V, and no obvious redox peaks were found in the negative scan. Interestingly, there are two groups of redox peaks for both BPC-3BTD and BPC-3BSe, located at 1.44 V/1.25 V, 1.18 V/1.02 V and 1.41 V/1.26 V and 1.18 V/1.01 V, respectively. It is worth mentioning that two redox peaks at −1.26 V/−1.39 V were found in the negative scan of BPC-3BSe. The different redox behaviours of four compounds suggested

Table 3 The fluorescence quantum yields of four compounds

Compounds	Φ_s	F_x	F_s	A_x	A_s	n_x	n_s	Φ_x
BPC-2BTD	0.38	50 893	38 253	0.038	0.038	1.42	1.34	0.57
BPC-2BSe	0.38	23 196	51 861	0.040	0.040	1.42	1.34	0.19
BPC-3BTD	0.38	33 083	51 861	0.039	0.039	1.42	1.34	0.27
BPC-3BSe	0.38	8263	50 541	0.037	0.037	1.42	1.34	0.07

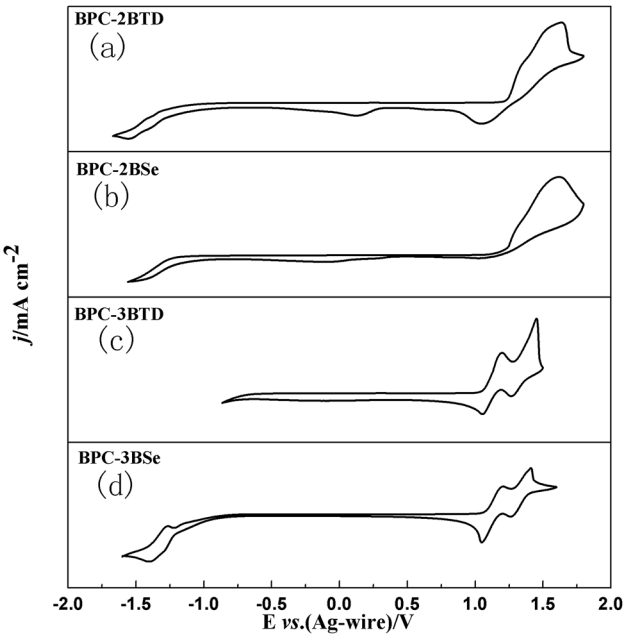

Fig. 3 CVcurves of BPC-2BTD (a), BPC-2BSe (b), BPC-3BTD (c) and BPC-3BSe (d).

that the substitution position and the type of acceptor have greatly influence on the properties of the compounds. The 3-position substitution has much lower oxidation potentials than that of the 2-position analogues, suggesting a higher degree of conjugation in the former compounds than the latter. The onset oxidation potentials of the compounds were gained from the corresponding tangent lines of the CV curves shown in Fig. 3. The values were 1.22 V, 1.20 V, 1.06 V and 1.05 V for BPC-2BTD, BPC-2BSe, BPC-3BTD and BPC-3BSe, respectively. BPC-2BSe had a lower onset oxidation potential than that of BPC-2BTD. The same phenomenon was observed between BPC-3BTD and BPC-3BSe. BPC-3BSe had a lower onset oxidation potential than that of BPC-3BTD, which suggested a higher HOMO level for the former compound than the latter. The HOMO levels of the compounds could be drawn from the following formula, HOMO = $-e(E_{onset} + 0.02 + 4.4)$,[38] and the HOMO energy levels of BPC-2BTD, BPC-2BSe, BPC-3BTD, and BPC-3BSe were calculated as −5.64 eV, −5.62 eV, −5.48 eV and −5.47 eV, respectively. It was suggested that the HOMO levels of the D–A type molecules could be reflected by the HOMO levels of the donor unit, as confirmed by the comparable HOMO values of the four compounds, since they have the same donor unit. According to the formula: LUMO = HOMO + E_g,[39,40] the LUMO energy levels of the four compounds were −3.05 eV, −3.17 eV, −3.00 eV and −3.14 eV, respectively, for BPC-2BTD, BPC-2BSe, BPC-3BTD and BPC-3BSe. Comparing the HOMO and LUMO values of four compounds, it was found that using BSe as the acceptor increased the energy levels of HOMO and decrease the energy levels of LUMO synchronously. Thus, the band gaps of the BSe-containing molecules are smaller than the BDT-containing analogues.

Moreover, substitution of the acceptor at the 3-position of the donor increased HOMO values and decrease LUMO values synchronously, also leading to the reduction of the band gap of the accordingly obtained molecule. The data for the electrochemical and optical properties of four compounds were summarized in Table 4.

Theoretical calculation

To obtain more accurate structural information for the molecules, quantum chemical computations of the compounds were undertaken. The theoretical values of E_g[d], HOMO[d] and LUMO[d] of four compounds are given in Table 4, which were obtained at the B3LYP/6-31G level employing the Gaussian 03 program.[23,26,35–38] The quantum chemical calculations were used to compare the theoretical values with the experimental results and to further understanding of the relationship between the molecule structure and its properties, as well as to gain a more intuitive display of the frontier orbital state of molecules. The HOMO and LUMO of the optimized molecular structures are shown in Fig. 4 (cartesian coordinates in ESI†). For optimized molecular structures, different substitution positions led to different planarities of the compounds with different HOMO and LUMO energy levels. Dihedral angles between the donor and acceptor are 31.78 and 32.95 for BPC-2BTD, 28.57 and 28.02 for BPC-3BTD, 34.92 and 33.87 for BPC-2BSe, and 31.23 and 30.65 for BPC-2BSe (Fig. 4). The introduction of the acceptor units (BTD or BSe) between the 3-position of two *N*-phenylcarbazole molecules generates a molecular system that has better coplanarity than the isomer obtained at the 2-position substitution. The distributions of π-electrons in the HOMO orbit of each of four molecules are mainly distributed on the *N*-phenylcarbazole donor unit, while the excited electron in the LUMO orbit of the four molecules was mainly distributed on the acceptor moieties, including benzothiadiazole and benzoselenadiazole. This indicates that ICT occurred from the ground state to the excited state.[22,26] The substitution position influenced the band gap significantly, but the changes from BTD to BSe as the acceptor unit had only a slight influence on the band gaps. Additionally, the 3-position substitution increased the HOMO value of the obtained compound. The replacement of BTD by BSe increased the HOMO and LUMO levels simultaneously. The HOMO and LUMO values obtained from the theoretical calculation are comparable with the data from experiments (Table 1), which further validated the correctness of the predicted molecular configuration as shown in Fig. 4.

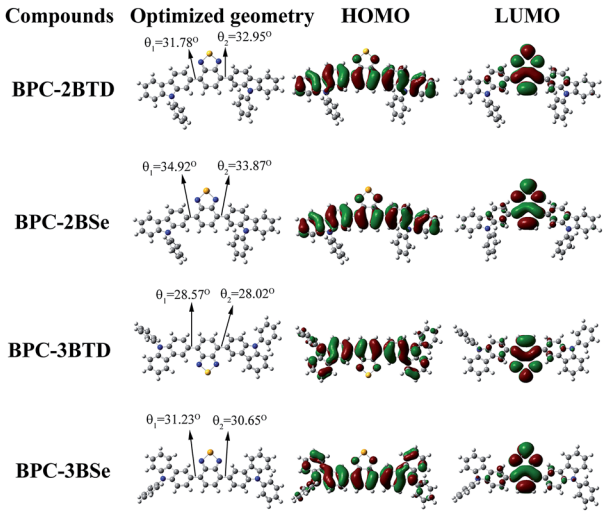

Fig. 4 Molecular orbital diagrams of HOMO and LUMO of four compounds.

Thermostability analysis

The thermal stabilities of four compounds were evaluated by thermogravimetric analysis (TGA). The TGA curves of BPC-2BTD is shown in Fig. 5, and the TGA curves of BPC-2BSe, BPC-3BTD and BPC-3BSe are presented in Fig. S5a–c in ESI.† These four compounds showed only a one-stage decomposition pattern, and the corresponding on-set degradation temperatures (T_d) reached 428 °C, 415 °C, 438 °C, and 418 °C, respectively. Differential thermal gravity (DTG) curves are also shown in Fig. 5 and S5a–c,† from which the maximum degradation rates of four compounds occurred at 525 °C, 469 °C, 511 °C and 464 °C, respectively. The data revealed the good thermal stability and high temperature resistance of these four compounds. Weight loss in the case of BPC-2BTD and BPC-3BTD was nearly 90%, whereas in the case of BPC-2BSe and BPC-3BSe, the weight losses were approximately 70% at 800 °C. The residues of BPC-2BSe and BPC-3BSe remained at approximately 30% of their original weight, higher than that of BPC-2BTD and BPC-3BTD. This might be due to the formation of SeO_2 during the decomposition of BPC-2BSe and BPC-3BSe. SeO_2 does not evaporate,

Table 4 The electrochemical and optical property data of compounds, include E_{onset}, λ_{max}, λ_{onset}, E_g, HOMO and LUMO

Compounds	E_{onset}, *vs.* (Ag-wire) (V)	λ_{max} (nm)/λ_{onset} (nm)	E_g[a] (eV)	HOMO[b] (eV)	LUMO[c] (eV)	E_g[d] (eV)	HOMO[d] (eV)	LUMO[d] (eV)
BPC-2BTD	1.22	318, 414/480	2.59	−5.64	−3.05	2.63	−5.51	−2.88
BPC-2BSe	1.20	327, 438/507	2.45	−5.62	−3.17	2.63	−5.46	−2.83
BPC-3BTD	1.06	298, 433/500	2.48	−5.48	−3.00	2.42	−5.21	−2.79
BPC-3BSe	1.05	299, 460/533	2.33	−5.47	−3.14	2.44	−5.18	−2.74

[a] Band gap calculated from λ_{onset}, $E_g = 1241/\lambda_{onset}$. [b] Calculated from onset oxidation potentials of the compounds, HOMO = $-e(E_{onset} + 0.02 + 4.4)$. [c] Estimated using empirical equations LUMO = HOMO + E_g. [d] E_g, HOMO and LUMO are calculated based on density functional theory (DFT).

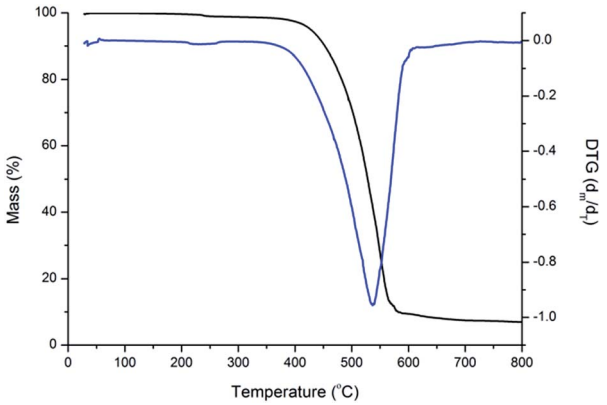

Fig. 5 TG and DTA curve of BPC-2BTD.

resulting in the increased observed residue in the thermograms.[41–44]

Conclusion

Four compounds (BPC-2BTD, BPC-2BSe, BPC-3BTD and BPC-3BSe) were synthesized based on Suzuki coupling reactions using benzocarbarzole as the donor and benzothiadiazole or benzoselenadiazole as the acceptor. The effects of the acceptor pattern and substitution position at the donor on the photoelectric properties of these compounds are discussed. The results demonstrate that substitution of the acceptor at the 3-position of *N*-phenylcarbazole is beneficial to the co-planarity of the obtained molecule reduced the band gaps of the molecules and caused a redshift in the emission spectra. At the same time, replacement of BTD by BSe as the acceptor unit could also reduce the band gap of the resultant molecule. All four compounds showed solvatochromism in different polar solvents. All four compounds had a high thermal stability and redox activities. In chloroform solution, BPC-2BTD, BPC-2BSe, BPC-3BTD and BPC-3BSe emitted green, yellowgreen, yellow and red lights upon irradiation, which are valuable primary colors. In summary, these four compounds are excellent luminescent materials and possess promising application prospects in the organic electroluminescence material fields.

Acknowledgements

The work was financially supported by the National Natural Science Foundation of China (51473074, 31400044), the Special Funds for Outstanding Young Innovative Talent Training plan of Guangdong Province (Seedling Project, 2013LYM_0105), and the Training program for Outstanding Young Teachers in Higher Education Institutions of Guangdong Province.

Notes and references

1 J. Peng, K. Q. Ye, J. B. Sun, Y. Zhan, J. H. Jia, P. C. Xue, G. H. Zhang, Z. Q. Zhang and R. Lu, *Dyes Pigm.*, 2015, **116**, 36–45.
2 D. Jiang, S. H. Chen, Z. Xue, Y. J. Li, H. B. Liu, W. S. Yang and Y. L. Li, *Dyes Pigm.*, 2016, **125**, 100–105.
3 L. Han, X. Y. Zu, Y. H. Cui, H. B. Wu, Q. Ye and J. R. Gao, *Org. Electron.*, 2014, **15**, 1536–1544.
4 R. D. Telore, A. G. Jadhav and N. Sekar, *J. Lumin.*, 2016, **179**, 420–428.
5 B. Huang, Z. H. Yin, X. X. Ban, W. Jiang, Y. Dai, J. Y. Zhang, Y. Y. Liu, Y. P. Yang and Y. M. Sun, *Dyes Pigm.*, 2015, **117**, 141–148.
6 E. Wincent, A. Kubota, A. T. Laragy, M. E. Jönsson, M. E. Hahn and J. Stegeman, *Biochem. Pharmacol.*, 2016, **110**, 117–129.
7 L. Fan, S. Q. Gao, Z. B. Li, W. F. Niu, W. J. Zhang, S. M. Shuang and C. Dong, *Sens. Actuators, B*, 2015, **221**, 1069–1076.
8 P. Ledwon, P. Zassowski, T. Jarosz, M. Lapkowski, P. Wagner, V. Cherpak and P. Stakhira, *J. Mater. Chem. C*, 2016, **4**, 2219–2227.
9 X. Wu, Z. Q. Guo, Y. Z. Wu, S. Q. Zhu, T. D. James and W. H. Zhu, *ACS Appl. Mater. Interfaces*, 2013, **5**, 12215–12220.
10 B. A. D. Neto, P. H. P. R. Carvalho and J. R. Correa, *Acc. Chem. Res.*, 2015, **48**, 1560–1569.
11 P. C. Li, H. Tong, J. Q. Ding, Z. Y. Xie and L. Wang, *J. Mater. Chem. A*, 2013, **1**, 8805–8812.
12 M. Paramasivam, A. Gupta, A. M. Raynor and S. V. Bhosale, *RSC Adv.*, 2014, **4**, 35318–35331.
13 P. C. Rodrigues, L. S. Berlim, D. Azevedo, N. C. S. Aavedra, P. N. Prasad, W. H. Schreiner, T. D. Z. Atvars and L. Akcelrud, *J. Phys. Chem. A*, 2012, **116**, 3681–3690.
14 C. Saravanan, S. Easwaramoorthi, C. Y. Hsiow, K. Wang, M. Hayashi and L. Wang, *Org. Lett.*, 2014, **16**, 354–357.
15 J. F. Wu, G. Q. Lai, Z. F. Li, Y. X. Lu, T. H. Leng, Y. J. Shen and C. Y. Wang, *Dyes Pigm.*, 2016, **124**, 268–276.
16 P. Thongkasee, A. Thangthong, N. Janthasing, T. Sudyoadsuk, S. Namuangruk, T. Keawin, S. Jungsuttiwong and V. Promarak, *ACS Appl. Mater. Interfaces*, 2014, **6**, 8212–8222.
17 S. S. Palayangoda, X. Cai, R. M. Adhikari and D. C. Neckers, *Org. Lett.*, 2008, **10**, 281–282.
18 A. Kimoto and Y. Tajima, *Org. Lett.*, 2012, **14**, 2282–2285.
19 O. Çimen, H. Dinçalp and C. Varlikli, *Sens. Actuators, B*, 2015, **209**, 853–863.
20 S. Yao, B. Kim, X. L. Yue, M. Y. C. Gomez and M. V. Bondar, *ACS Omega*, 2016, **1**, 1149–1156.
21 J. L. Wang, Q. Xiao and J. Pei, *Org. Lett.*, 2010, **12**(18), 4164–4167.
22 P. B. Pati and S. S. Zade, *Cryst. Growth Des.*, 2014, **14**, 1695–1700.
23 S. Mondal, M. Konda, B. Kauffmann, M. K. Manna and A. K. Das, *Cryst. Growth Des.*, 2015, **15**, 5548–5554.
24 S. Toksabay, S. O. Hacioglu, N. A. Unlu, A. Cirpan and L. Toppare, *Polymer*, 2014, **55**, 3093–3099.
25 F. B. Koyuncu, E. Sefer, S. Koyuncu and E. Ozdemir, *Polymer*, 2011, **52**, 5772–5779.
26 M. Akbayrak and A. M. Önal, *Polym. Chem.*, 2016, **7**, 6110–6119.
27 Z. H. Guo, T. Lei, Z. X. Jin, J. Y. Wang and J. Pei, *Org. Lett.*, 2013, **15**, 3530–3533.

28 D. Baran, G. Oktem, S. Celebi and L. Toppare, *Macromol. Chem. Phys.*, 2011, **212**, 799–805.
29 E. J. Zhou, J. Z. Cong, K. Hashimoto and K. Tajima, *Macromolecules*, 2013, **46**, 763–768.
30 F. F. Zhang, C. H. Zhou and J. P. Yan, *Chin. J. Org. Chem.*, 2010, **30**(6), 783–796.
31 X. F. Lu, S. H. Fan, J. H. Wu, X. W. Jia, Z. S. Wang and G. Zhou, *J. Org. Chem.*, 2014, **79**, 6480–6489.
32 T. Ishi-i, M. Sakai and C. Shinoda, *Tetrahedron*, 2013, **69**, 9475–9480.
33 J. L. Westrup, L. W. Oenning, M. M. S. Paula, R. C. Duarte, F. S. Rodembusch, T. E. A. Frizon, L. Silva and A. G. Dal-Bó, *Dyes Pigm.*, 2016, **126**, 209–217.
34 M. D. Damaceanu, C. P. Constantin and L. Marin, *Dyes Pigm.*, 2016, **134**, 382–396.
35 T. E. A. Frizon, J. C. V. Martínez, J. L. Westrup, R. C. Duarte, E. Zapp, K. G. Domiciano, F. S. Rodembusch and A. G. Dal-Bó, *Dyes Pigm.*, 2016, **135**, 26–35.
36 G. J. Huang, J. H. Ho, C. Prabhakar, Y. H. Liu, S. M. Peng and J. S. Yang, *Org. Lett.*, 2012, **14**, 5034–5037.
37 M. Onoda, S. Uchiyama, T. Santa and K. Imai, *Anal. Chem.*, 2002, **74**, 4089–4096.
38 S. Uchiyama, Y. Matsumura, A. P. de Silva and K. Iwai, *Anal. Chem.*, 2003, **75**, 5926–5935.
39 E. Sefer, H. Bilgili, B. Gultekin, M. Tonga and S. Koyuncu, *Dyes Pigm.*, 2015, **113**, 121–128.
40 J. K. Xu, H. T. Liu, S. Z. Pu, F. Y. Li and M. B. Luo, *Macromolecules*, 2006, **39**, 5611–5616.
41 L. Benati, P. C. Montevecchi and G. Zanardi, *J. Org. Chem.*, 1977, **42**, 575–577.
42 S. Lu, M. Yang, J. Luo, Y. Cao and F. Bai, *Macromol. Chem. Phys.*, 2005, **206**, 664–671.
43 A. M. Alsalme, A. A. B. Alghamdi, A. A. G. Q. Alhamdani and A. Iraqi, *Int. J. Electrochem. Sci.*, 2014, **9**, 1920–1941.
44 S. Wen, J. Pei, Y. Zhou, P. Li, L. Xue and Y. Li, *Macromolecules*, 2009, **42**, 4977–4984.